# Physical model of acoustic forward scattering by cylindrical shell and its experimental validation*

Lei Bo(雷 波)†, Yang Kun-De(杨坤德), and Ma Yuan-Liang(马远良)

*College of Marine, Northwestern Polytechnical University, Xi'an* 710072, *China*

(Received 13 September 2009; revised manuscript received 23 October 2009)

Research on the underwater target scattering can provide important theoretical support for target detection. The scattering model of cylindrical shell is established in this paper. It is found that the forward target strength is much stronger and varies with angles of incident wave less significantly than backward target strength. The received forward signal strength fluctuates with the target moving due to the interference between direct signal and scattering signal, which is most significant when the target approaches the baseline. An experiment is carried out in an anechoic tank to validate the scattering model. The method of acquisiting forward scattering in the tank is proposed. The forward and the backward target strengths are achieved by using the pulse compression technology, and they are about 3dB less than the modeling results. The forward scattering phenomena of quiescent and moving targets are measured, which are similar to modeling results with different target types.

**Keywords:** scattering model, forward scattering, target strength, shell

**PACC:** 4330

## 1. Introduction

In the past few years, the acoustic scattering models of underwater target were adequately developed.[1−5] These models accord well with the real scattering of underwater target. Ye[3] assumed a differential element of the cylinder scattered sound to be part of an infinite cylinder of the same radius, thus the scattering function of cylinder body was derived rigorously by using the Kirchhoff integral theorem. The method is useful for studying the target scattering near beam aspect. Virtual source method[4] has advantage in acoustical scattering calculation when target is under a complex environment, but the computation of method is a burden in the case of large target compared with wavelength. It was found that the forward target strength was much stronger than the backward target strength, so the target detection with forward scattering was attractive[6−10] recently. Some relevant studies were conducted, such as modeling the forward scattering in the shallow water waveguide,[6,7] detecting target with continuous wave[8,9] and the structure of arrival with target submerged.[10] However, these studies were focused mainly on the target detection in the shallow water with forward scattering. The physical principle of the forward scattering by underwater target is rarely studied, and the relevant laboratory experiment is hardly carried out either. The true reason is that the forward scattering signal and the direct arrival signal arrive at the forward hydrophone at the same time, and the acquisition of forward scattering signal is difficult due to the strong interference of direct signal.

In the experiments of monostatic sonar,[11,12] the environment and the target shape in reality were considered in the measurement of monostatic target strength. However, due to the complex bistatic reverberation[13] and dispersive propagation[14] in the shallow water, the measurements of forward scattering were still restricted in the laboratory.[15,16] Especially there has been almost no published report on the forward scattering by large target. Use of forward scattering may enjoy a few advantages. First, as will be seen below, the forward target strength is much stronger than the backward target strength. Second, the forward scattering of target varies with the incidence angle of sound less significantly than backward scattering. In real situations where the target moves and the incidence angle changes with time, the forward scattering signal is changed insignificantly.

*Project supported by the National Natural Science Foundation of China (Grant No. 10774119), the program for New Century Excellent Talents in University, China (Grant No. NCET-08-0455), the Natural Science Foundation of Shaanxi province, China (Grant No. SJ08F07), the Foundation of National Laboratory of Acoustics, and the Northwestern Polytechnical University NPU Foundation for Fundamental Research, China (Grant No. 2007004).

†Corresponding author. E-mail: lei.bo.thunder@gmail.com

© 2010 Chinese Physical Society and IOP Publishing Ltd

Therefore the detection method based on the forward scattering is stable with respect to the change in target moving direction.

The scattering model of cylindrical shell is derived in this paper, and a simple laboratory experiment is designed and carried out in the anechoic tank to observe the scattering phenomenon. The forward and the backward target strengths of cylindrical shell insonified by 30 kHz acoustical wave are calculated and measured. The forward target strength is 12dB higher than the backward target strength, and 3dB less than the modeling results. The reasons are studied in the paper. The effects of forward scattering by moving target are analysed, and the general physical principles are achieved.

## 2. Scattering model

The scattering by finite cylindrical shell is illustrated in Fig. 1. The length of the shell is $L$ with outer radius $a$ and inner radius $b$. The angles between the incident plane wave and axis of cylinder, and between the scattering wave and axis of cylinder, are $\theta_{\rm i}$ and $\theta_{\rm s}$, respectively.

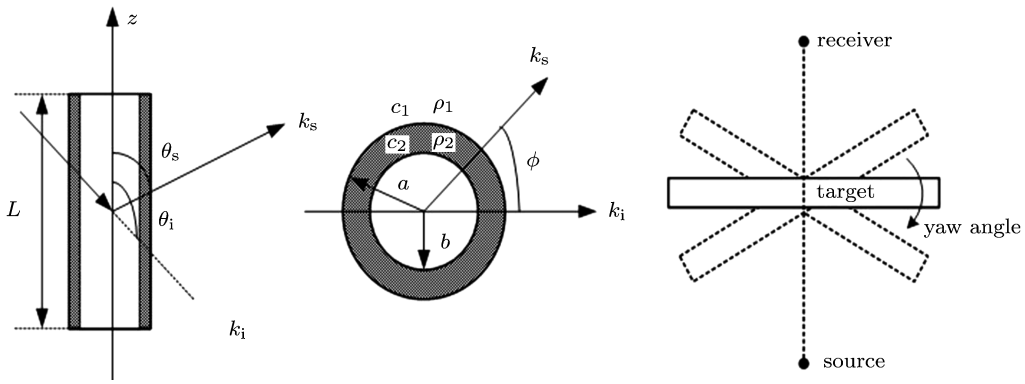



**Fig. 1.** Illustration of scattering by finite cylindrical shell.

The yaw angle with respect to the beam direction is 0°. The incident plane wave is represented as the sum of cylindrical wave,[17]

$$p_{\rm i} = {\rm e}^{{\rm i}\,kz\cos\theta_{\rm i}} \sum_{n=0}^{\infty} {\rm i}^n \varepsilon_n {\rm J}_n(k_1 r\sin\theta_{\rm i})\cos(n\phi), \qquad (1)$$

where $\varepsilon_n = \begin{cases} 1, & n = 0, \\ 2, & n = 1, 2, 3, \cdots. \end{cases}$ The scattering field of cylinder is written as

$$p_{\rm s} = {\rm e}^{{\rm i}\,kz\cos\theta_{\rm i}} \sum_{n=0}^{\infty} B_n {\rm H}_n(k_1 r\sin\theta_{\rm i})\cos(n\phi). \qquad (2)$$

The acoustic character of the shell is considered only for modeling the target strength. The internal field of the shell is

$$p_{\rm int} = {\rm e}^{{\rm i}\,kz\cos\theta_{\rm i}} \sum_{n=0}^{\infty} [A_n {\rm J}_n(k_2 r\sin\theta_{\rm i}) + C_n {\rm H}_n(k_2 r\sin\theta_{\rm i})]\cos(n\phi), \qquad (3)$$

where $A_n$, $B_n$ and $C_n$ are the coefficients determined by the boundary conditions of the shell scattering; ${\rm J}_n$ and ${\rm H}_n$ denote the Bessel function and the first kind Hankel function, respectively; $k_1$ and $k_2$ are wavenumbers in the water volume and shell material, respectively.

The shell is full of air. It approximately satisfies the soft boundary condition on the inner surface of shell, i.e. the pressure is zero on the inner surface,

$$p_{\rm int}|_{r=b} = {\rm e}^{{\rm i}\,kz\cos\theta_{\rm i}} \sum_{n=0}^{\infty} [A_n {\rm J}_n(k_2 r\sin\theta_{\rm i}) + C_n {\rm H}_n(k_2 r\sin\theta_{\rm i})]\cos(n\phi)|_{r=b} = 0. \qquad (4)$$

Thus the coefficient $C_n$ is achieved to be

$$C_n = -\frac{{\rm J}_n(k_2 b\sin\theta_{\rm i})}{{\rm H}_n(k_2 b\sin\theta_{\rm i})} A_n. \qquad (5)$$

The pressure and velocity on the surface of shell are continuous, so

$$B_n = D_{1n}/D_{2n}, \qquad (6)$$

where

$$
\begin{aligned}
D_{1n} = &-\mathrm{i}^n \varepsilon_n [g\mathrm{J}'_n(k_1 a\sin\theta_\mathrm{i})\mathrm{J}_n(k_2 a\sin\theta_\mathrm{i}) \\
&- \mathrm{J}_n(k_1 a\sin\theta_\mathrm{i})\mathrm{J}'_n(k_2 a\sin\theta_\mathrm{i}) \\
&- \beta(g\mathrm{J}'_n(k_1 a\sin\theta_\mathrm{i})\mathrm{H}_n(k_2 a\sin\theta_\mathrm{i}) \\
&- \mathrm{J}_n(k_1 a\sin\theta_\mathrm{i})\mathrm{H}'_n(k_2 a\sin\theta_\mathrm{i}))], \\
D_{2n} = &\, g\mathrm{H}'_n(k_1 a\sin\theta_\mathrm{i})\mathrm{J}_n(k_2 a\sin\theta_\mathrm{i}) \\
&- \mathrm{H}_n(k_1 a\sin\theta_\mathrm{i})\mathrm{J}'_n(k_2 a\sin\theta_\mathrm{i}) \\
&- \beta(g\mathrm{H}'_n(k_1 a\sin\theta_\mathrm{i})\mathrm{H}_n(k_2 a\sin\theta_\mathrm{i}) \\
&- \mathrm{H}_n(k_1 a\sin\theta_\mathrm{i})\mathrm{H}'_n(k_2 a\sin\theta_\mathrm{i})), \\
\beta = &\frac{\mathrm{J}_n(k_2 b\sin\theta_\mathrm{i})}{\mathrm{H}_n(k_2 b\sin\theta_\mathrm{i})}, \quad \text{and} \quad g = \frac{k_1\rho_2}{k_2\rho_1}.
\end{aligned}
$$

The scattering function of finite cylinder near beam aspect can be derived rigorously by using the Kirchhoff integral theorem.[3] It is written as

$$
f(\theta_\mathrm{i},\theta_\mathrm{s},\phi) = \frac{-\mathrm{i}\,L}{\pi}\mathrm{sinc}\Delta\sum_{n=0}^{\infty} B_n F_n(-\mathrm{i})^n\cos(n\phi), \quad (7)
$$

where

$$
\mathrm{sinc}\Delta = \frac{\sin(k_1 L(\cos\theta_\mathrm{s}-\cos\theta_\mathrm{i})/2)}{k_1 L(\cos\theta_\mathrm{s}-\cos\theta_\mathrm{i})/2}, \quad (8)
$$

$$
\begin{aligned}
F_n = &\frac{\pi}{2\,\mathrm{i}}(ka)[\mathrm{H}'_n(k_1 a\sin\theta_\mathrm{i})\mathrm{J}_n(k_1 a\sin\theta_\mathrm{s})\sin\theta_\mathrm{i} \\
&- \mathrm{H}_n(k_1 a\sin\theta_\mathrm{i})\mathrm{J}'_n(k_1 a\sin\theta_\mathrm{s})\sin\theta_\mathrm{s}]. \quad (9)
\end{aligned}
$$

According to Eqs. (6)–(9), the target strength is determined to be

$$
\mathrm{TS} = 20\mathrm{lg}\,|f(\theta_\mathrm{i},\theta_\mathrm{s},\phi)|\,. \quad (10)
$$

In the simulation, a cylindrical shell with 70 cm in length, 10.95 cm in outer radius and 0.6 cm in thickness is considered. The sound speed of water is 1500 m/s, and the mass density of water is 1.0 g/cm$^3$. The shell is made of steel with sound speed 4900 m/s, and density 7.8 g/cm$^3$. The inner of the shell is in vacuum. The distribution of forward target strength insonified by 30 kHz acoustic wave is shown in Fig. 2(a), where the horizontal axis denotes the yaw angle of target. The forward target strength decreases 3 dB at target yaw angle 45°, which means that the change of forward target strength is kept within 3 dB with target yawing near beam aspect. When the angle is larger than 45°, the yaw angle has a great influence on forward target strength. In the backward direction as shown in Fig. 2(b), the target strength can only achieves −4 dB, even if in the reflecting direction of incident wave. While in the other directions, the target strength drops off significantly. The yaw angle of target has a great influence on the backward target strength.

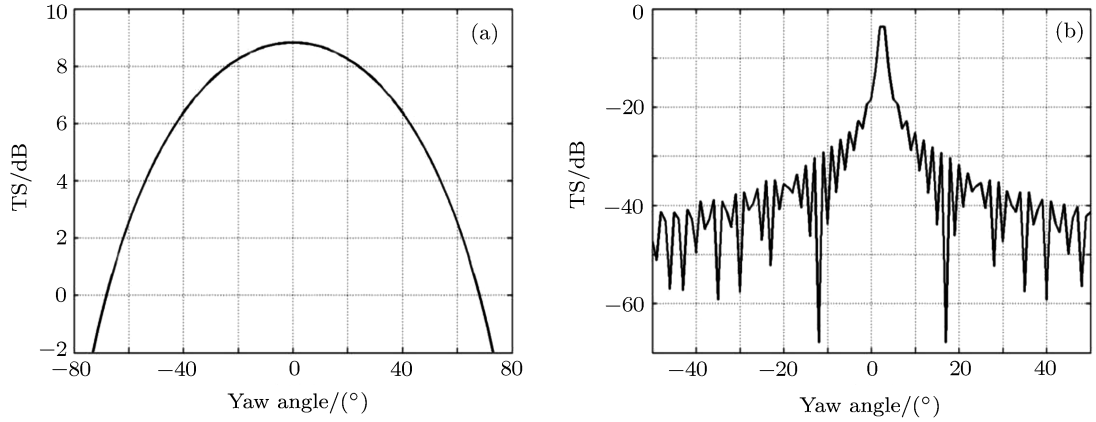



**Fig. 2.** Distributions of forward (a) and backward (b) target strengths with respect to the yaw angle of target.

The forward scattering function of the cylindrical shell is shown in Fig. 3. The horizontal axis denotes the angle of scattering. Figures 3 (a) and 3(b) are the strength and the phase of the forward scattering, respectively. In the forward direction, the function has a maximum value and the target strength is strongest. The forward scattering occupies a sector whose width is in inverse proportion to $k_1 L$. The phase of the forward scattering function is variable alternatively. The difference in phase between the forward scattering signal and direct signal is changed with target position. The forward scattering signal interferes with direct signal so that the Poisson spot is generated on the plane vertical to the incident direction, which is similar to the spheroid scattering.[5] When the target moves with respect to baseline, the amplitude and the phase of the received signal

are changed due to the present of Poisson spot. The acoustical shadow zone is generated in near field because of the destructive interference between forward scattering signal and direct signal when target passes through the baseline.

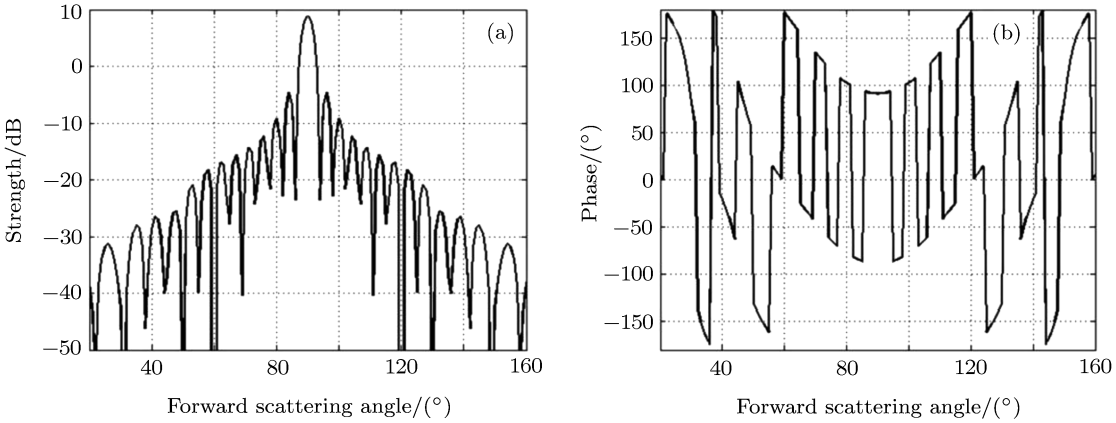



**Fig. 3.** Curves for strength (a) and phase (b) of forward scattering of cylindrical shell versus forward scattering angle.

The solid line in Fig. 4 denotes the variation of received signal amplitude with the cylindrical shell perpendicular to the baseline in the far field. The amplitude of incident plane wave is 1 V. And the moving speed of target is 0.15 m/s with a 50 m distance to hydrophone when target passes through the baseline at the time moment 20 s. The duration of continuous signal is 40 s. When the target approaches the baseline, the received signal strength fluctuates significantly. In the far field, the received signal becomes stronger because of the superposition of the forward scattering signal and direct signal. The received signal fluctuates less significantly when target departure from the baseline, which is because of the sidelobe effect of the forward scattering. A rigid plate is presented here for comparison. The size of the plate is 1 m×1 m. And the result is shown by dash line in Fig. 4.

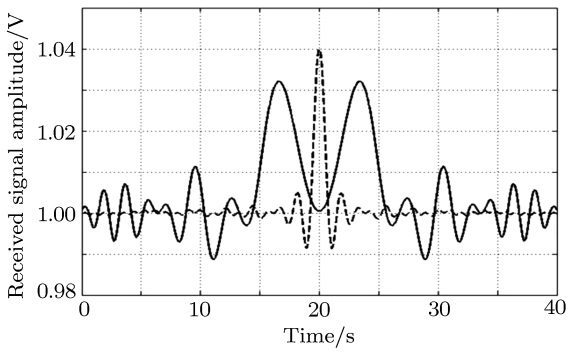



**Fig. 4.** Fluctuations of received signal amplitude due to target moving in the far field, where solid line and dash lines denote cylindrical shell and rigid plate, respectively.

The signal strength also fluctuates significantly when target approaches the baseline, even though the different targets have different forward scattering functions and forward scattering signals. It is difficult to model the scattering in the near field because the scattering function in Eq. (7) is only hold in the far field.

# 3. Laboratory experiment

## 3.1. Experimental setup

The experiment is carried out in an anechoic water tank, which has a cone-shaped sound absorber on the wall of tank and water surface. The frequency band of the absorber is 2–80 kHz. The aim of the experiment is to observe the scattering phenomenon of cylindrical shell and the effect of forward scattering. The scattering of underwater large target is difficult to measure directly, so a scaled model is used. The scaling coefficient is about 100. Thus the frequency is up to 30 kHz.

The experimental setup is shown in Fig. 5(a). The transmitter with 20° (−3 dB) beamwidth is fixed at a depth of 2 m underwater and works at a central frequency of 30 kHz. The centre of the target is on the axis of source beam pattern. And the measured sound speed is 1483 m/s. All the hydrophones are at a depth of 2 m. The echoes from the surface of water and walls of tank are very weak. Two types of hydrophones are used. No. 2 and No. 3 are type ST500, No. 6 is F4032, with sensitivities of −191 dB and −160 dB at 30 kHz, respectively. The maximum amplitude outputs of these hydrophones are 10 V.

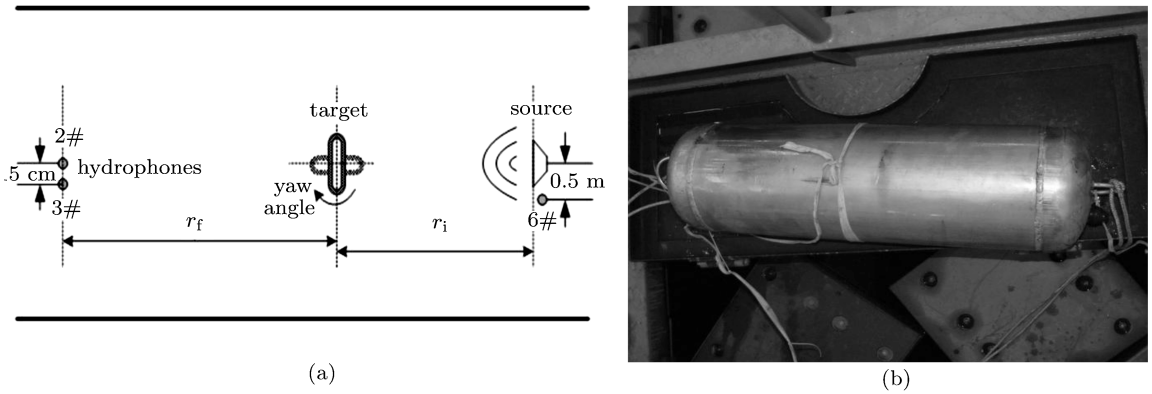



**Fig. 5.** Diagram of the experiment, where panel (a) shows experimental configuration and panel (b) displays the shape of the cylindrical shell.

The bandwidth of the bandpass filter is 2 kHz, with a central frequency 30 kHz. And the sample frequency is set to be 200 kHz.

The cylindrical shell is made of stainless steel with air filled. As shown in Fig. 5(b), the shell is 0.6 cm thick, 70 cm long, and has an outer radius of 10.95 cm. Each of the ends has a spherical cap. The target is softly fixed with lines under the platform. The minimum scale angle of the platform is 1°. The target drops about 3 cm in the experiment because of the gear clearance, which is much smaller than the size of target and has a negligible influence on the measured results.

## 3.2. Measurement principles

Given the design of the experiment, the forward and backward target strength can be derived straightforwardly. The wavelength is much smaller than the size of target. When the target is close to the transmitter, the Fresnel (phase) zones should be considered. The radius of the first Fresnel zone in the case of forward scattering of far field can be expressed as[16]

$$a = \sqrt{\lambda r_{\rm i} r_{\rm f}/r_{\rm d}}, \tag{11}$$

where $\lambda$ is the wavelength; $r_{\rm i}$ and $r_{\rm f}$ are the distances from source to target, and from target to forward hydrophone, respectively. $r_{\rm d} = r_{\rm i} + r_{\rm f}$ is the distance from source to hydrophone. If the target is not entirely within the first Fresnel zone, the scattering signals from the first and second zones tend to interfere destructively. In this experiment, $r_{\rm i} = 5.3$ m, $r_{\rm f} = 8.8$ m, and $r_{\rm d} = 14.1$ m. Thus $a$ is 0.41 m at frequency 30 kHz. The size of first Fresnel zone is larger than the 70-cm-long target in the far field. It means that the entire target is in the first Fresnel zone at frequency 30 kHz. The wave insonifying the target can be considered as a plane wave coming from a certain direction.

The method given in Ref. [15] is adopted to measure the target strength. The target is on the central axis of the source beam, and the beam pattern of the source can be omitted. The incident wave on the target ($p_{\rm i}$) and the direct wave on the hydrophone ($p_{\rm d}$) can be written as

$$p_{\rm i} = P_0/r_{\rm i} \cdot {\rm e}^{-{\rm j}kr_{\rm i}}, \quad p_{\rm d} = P_0/r_{\rm d} \cdot {\rm e}^{-{\rm j}kr_{\rm d}}, \tag{12}$$

and the forward scattering wave in the far field ($p_{\rm f}$) as

$$\begin{aligned} p_{\rm f} &= p_{\rm i}/r_{\rm f} \cdot {\rm e}^{-{\rm j}kr_{\rm f}} \cdot F = P_0/r_{\rm i}r_{\rm f} \cdot F \cdot {\rm e}^{-{\rm j}k(r_{\rm i}+r_{\rm f})} \\ &= P_0/r_{\rm i}r_{\rm f} \cdot F \cdot {\rm e}^{-{\rm j}kr_{\rm d}}, \end{aligned} \tag{13}$$

where $P_0$ is the pressure amplitude at 1-m distance from the source. $F$ is the forward scattering function of the target. Equations (12) and (13) lead to

$$p_{\rm f} = p_{\rm d}\frac{r_{\rm d}}{r_{\rm i}r_{\rm f}} \cdot F. \tag{14}$$

It is clear from this equation that there is difference in phase between the forward scattering signal and direct signal determined by the forward scattering function. The amplitude of forward scattering function is expressed as

$$|F| = \frac{P_{\rm f}}{P_{\rm d}} \cdot \frac{r_{\rm i}r_{\rm f}}{r_{\rm d}}, \tag{15}$$

where $P_{\rm f}$ and $P_{\rm d}$ represent the forward and the direct signal amplitudes, respectively. According to Eq. (15), the measurements of the forward scattering function have no direct relationship with the sensitivity of hydrophone.

In the forward direction of the target, the forward scattering signal and the direct signal arrive at the hydrophone at the same time. The direct signal must be subtracted from the received signal. The direct signals with and without target can be regarded as the same in amplitude and phase under this static laboratory environment, so the pulse compression technology[18]

is used. The received signals with and without target are synchronized, so that the direct signals under these two cases arrive at the same time in the sampled signal sequence. The difference between these two received signals is the forward scattering signal. In the aforementioned procedure, the hydrophone is assumed to be aligned with the centre of the source beam pattern. If that is not satisfied, Eq. (14) does not hold and the amplitude of forward scattering function is only achieved from Eq. (15).

According to the definition of target strength,[19] the forward target strength is expressed as

$$\mathrm{TS} = 20\lg(P_\mathrm{f}/P_\mathrm{i})|_{r_\mathrm{ref}} = 20\lg|F||_{r_\mathrm{ref}} \qquad (16)$$

where $r_\mathrm{ref} = 1$ m (from the acoustical centre of target).

So far we have assumed that the target is on the beam axis. If it deviates slightly, the results can be corrected by dividing Eq. (15) by $D(\theta)$, where $D(\theta)$ is the beam pattern of the source and $\theta$ the angle of target deviating from the beam axis.

The length of target is $L$. The incident angle with respect to the axis of the cylinder is $\theta$ and sound speed in water is $c$. For monostatic measurement of target strength, the pulse duration contributing to target strength is

$$\tau_0 = 2L\cos\theta/c. \qquad (17)$$

When the transmitted pulse duration $\tau$ is longer than $\tau_0$, the target is fully insonfied by the pulse at angle $\theta$. In other words, when the angle $\theta$ is larger than

$$\theta_0 = \cos^{-1}(c\tau/2L), \qquad (18)$$

the measured target strength is correct.

## 3.3. Results and discussion

### 3.3.1. Backward target strength

The target is located at a depth of 1.5 m under the water surface. The 30 kHz pulse signals with durations of 5 cycles and 20 cycles are transmitted separately. And the data of No. 6 hydrophone is processed. According to Eq. (18), the valid intervals of yaw angle are $[-10°, 10°]$ and $[-45°, 45°]$, respectively. At angles that are beyond these intervals, the echoes from the end-caps of cylindrical shell are distinguished clearly. The results are shown in Fig.6, obtained by utilizing the pulse compression method.

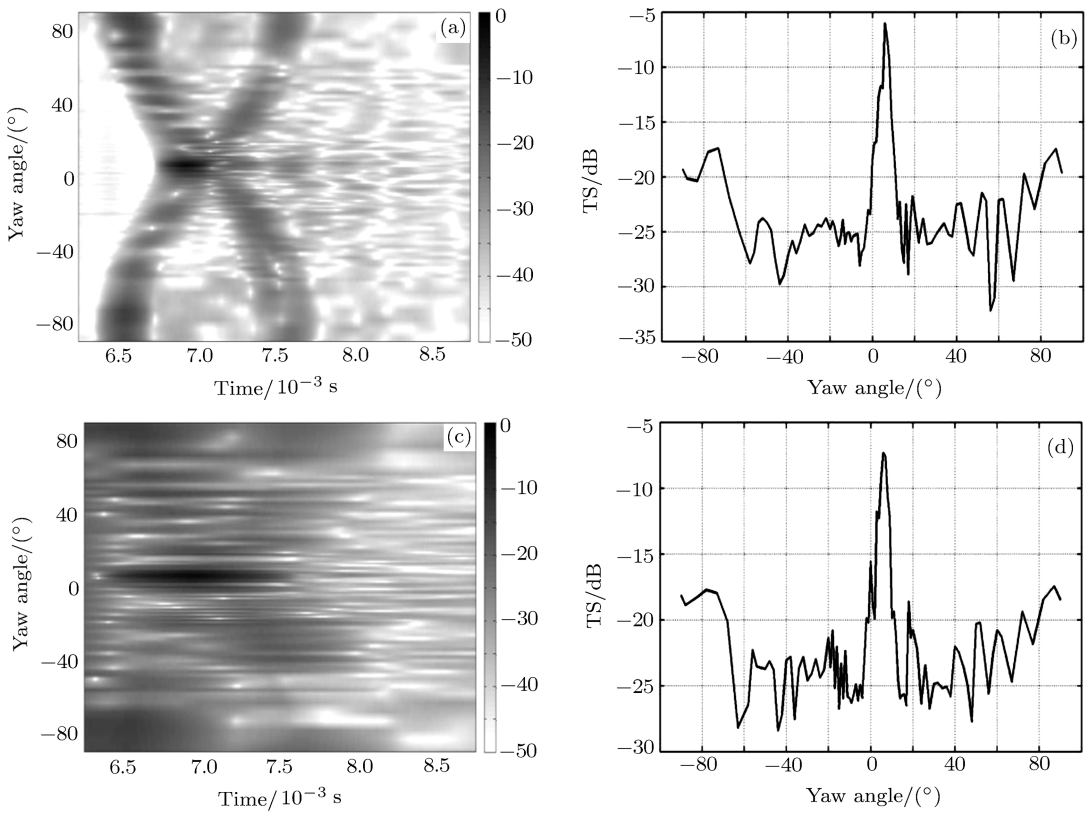



**Fig. 6.** Backward echoes and target strengths. Panels (a) and (c) show that the signal arriving structure with target yawing, and panels (b) and (d) display the backward target strengths with target yawing. In panels (a) and (b) a 5-cycle pulse is used, while in panels (c) and (d) a 20-cycle pulse is adopted.

Figures 6(a) and 6(b) are the results acquired with a 5-cycle signal, Figs. 6(c) and 6(d) with a 20-cycle signal. It can be seen from Fig. 6(a) that the arriving times of echoes change with target yawing. The echosignals from beam aspect of the target are later but stronger than those reflected from the two end-caps. This is because the two end-caps are closer to hydrophone than to the beam aspect when the target yaws. The target strength at beam aspect is strongest with a largest reflect cross section. Figure 6(b) shows the backward target strength versus target yaw angle. The target strength approaches to the strongest value (−6 dB) at a yaw angle of about 5°, which is because the hydrophone is deviated by 0.5 m from the axis of source. When the yaw angle becomes large, the target strength drops off quickly. And the target strength is acquired from the first echoes beyond the valid interval [−10°, 10°], which denotes the strength of the nearest spot of target to receiver. While in Fig. 6(c), the long pulse is used, thus the entire target is insonified by incident signal in [−45°, 45°]. As shown in Fig. 6(d), the target strength at yaw angle 5° is about −6.2 dB, a little smaller than the results from 5-cycle signal. It is the same as the mentioned above, the target strength is only the spot strength of target beyond the aspect interval [−45°, 45°].

### 3.3.2. Forward target strength

When the target is on the baseline between the source and receiver, the acoustical shadow zone is generated in the near field, the received signal strength is decreased. The direct signal interferes with the forward scattering signal and needs to be subtracted. It can be seen from the top of Fig. 7(a) that the amplitude of direct signal is about 1.5 V without target. When the target is located between the source and the receiver, the forward scattering signal and the direct signal interfere destructively and the amplitude of received signal drops to 0.8 V. After the direct signal is subtracted by using the subtraction method proposed in this paper, the forward scattering signal is obtained as shown in the bottom of Fig. 7(a). The difference in phase between the direct and the forward scattering signals shown in Fig. 7(a) is 157°, which tends to interfere destructively. This is consistent well with the observation.

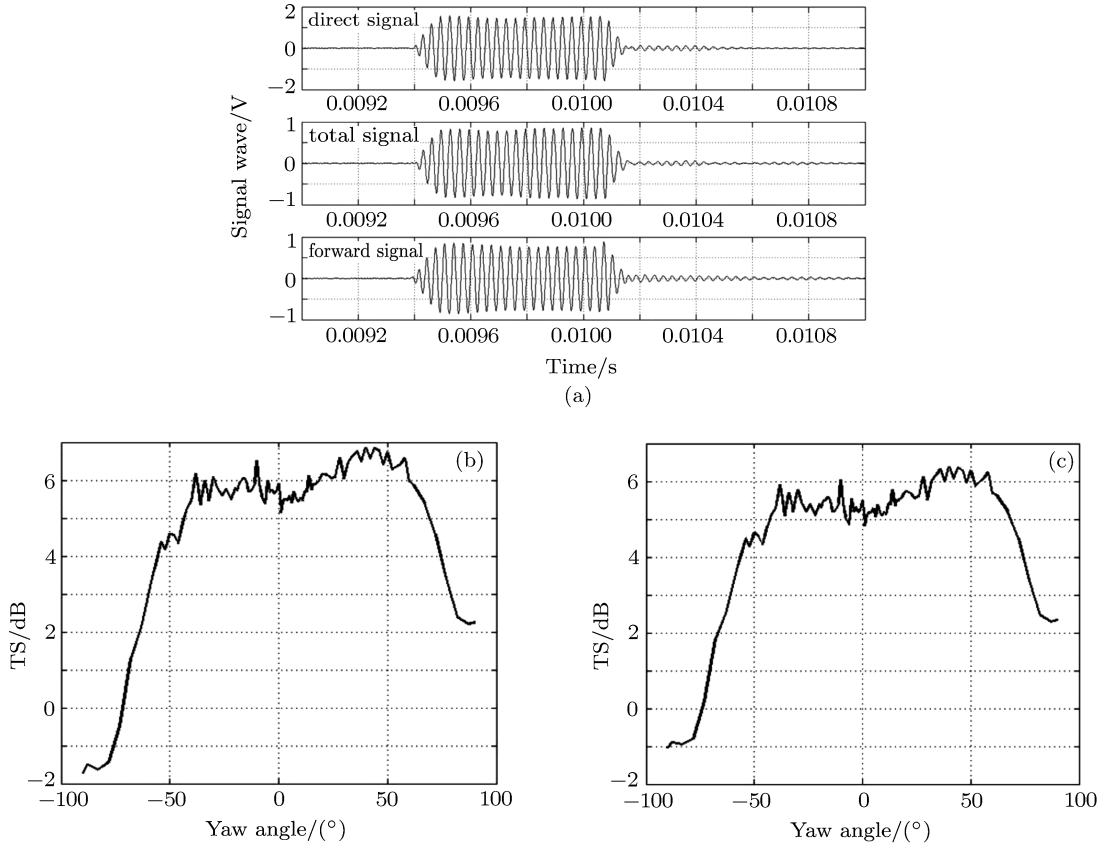



**Fig. 7.** Forward scattering signal and the distribution of forward target strength. Panel (a) shows the received and scattering signals of No. 2 hydrophone with and without targets; panel (b) displays the forward target strength obtained by No. 2 hydrophone; panel (c) exhibits the forward target strength obtained by No. 3 hydrophone.

From Eqs. (5) and (6), the forward target strength is obtained. The distribution of forward target strengths with target yawing is shown in Figs. 7(b) and 7(c) after averaging 8 times, where the 20-cycle transmitted signal is used. The forward target strength is strongest in the beam aspect with a largest cross section. When the yaw angle is greater than 50°, the forward target decreases. In Fig. 7(c), No. 3 hydrophone is deviated by 0.15 m from the beam axis, which leads the forward target strength to be 0.3 dB less than the result of No. 2 hydrophone. Comparing Figs. 6 and 7 shows that the forward target strength is 12 dB higher than the backward target strength, and varies less significantly with target yawing. Thus the detection method based on the forward scattering is stable with respect to the change of target moving direction.

The measurement results are compared with model results in Fig. 2, showing that the backward target strength and the forward target strength are about 2.2 dB and 2 dB lower than the model result respectively. The main reasons are as follows. (i) The model target is different from real target: the target in the experiment is not an absolutely homogenous cylindrical shell. (ii) The distance between the hydrophones and the target is less than $L^2/\lambda$. The transmission loss behaves like cylindrical expansion in near field and spherical expansion in far field. If the spherical expansion is considered in target strength calculation of near field, the target is smaller than that of far field.[20]

### 3.4. Forward scattering of continuous wave

The above simulation shows that the strength of forward received signal is fluctuated with target moving because of the interference between the forward scattering signal and the direct signal. Here the continuous wave is transmitted, and the targets move vertically in the tank. The effects of the forward scattering signal are observed.

When there is no target, the amplitude of received signal is 1.1 V. Then the cylindrical shell is submerged into the tank and moves vertically. The speed is about 0.15 m/s. The strengths of the received signal are shown in Fig. 8.

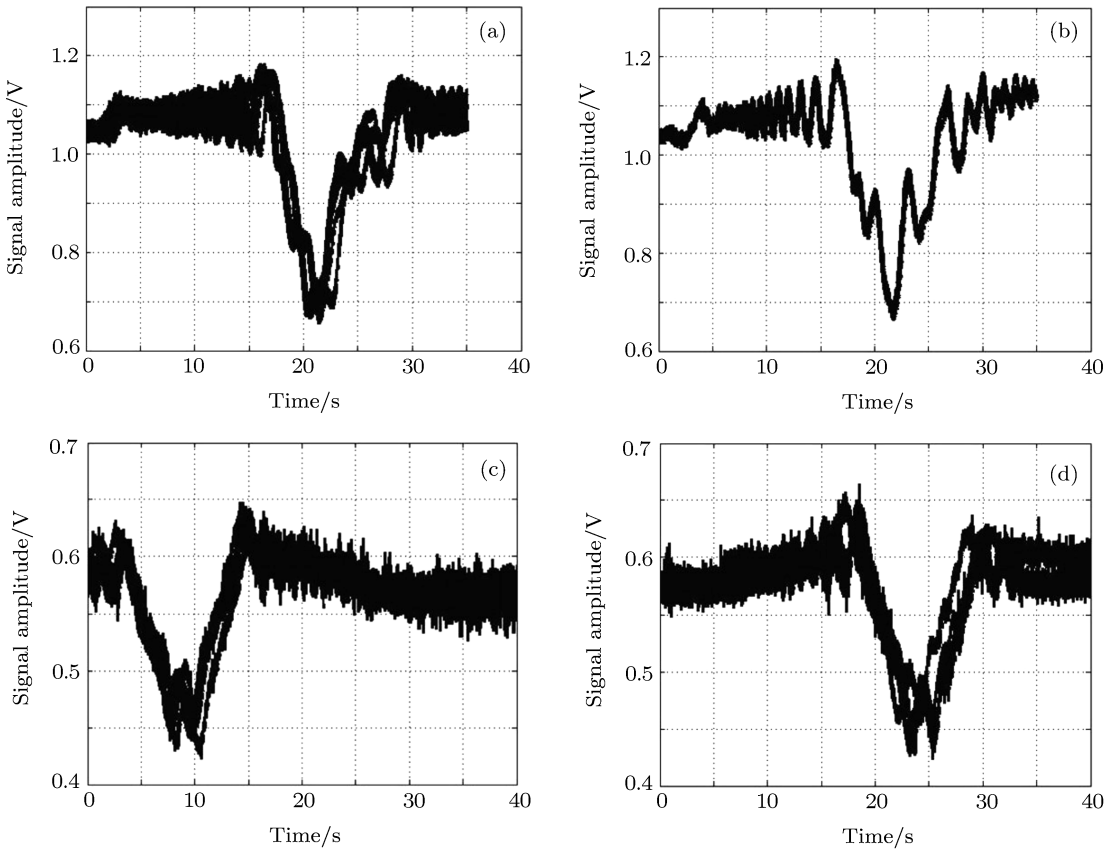



**Fig. 8.** Fluctuations of received amplitude with target moving vertically. Panel (a) shows that the trajectory is deviated by 0.27m from the baseline with target up-moving; panel (b) displays that the target crosses the baseline with target up-moving; panels (c) and (d) exhibit the cases of the plate moving down and up respectively.

In Fig. 8(a), the trajectory is deviated by 0.27 m from the baseline, and target moves cross the baseline in Fig. 8(b). It can be seen that at about time moment 22 s, the received signal is weakest, and the target, the source and the hydrophone are at the same depths at this time. The acoustical shadow zone is generated in the forward direction. The strength of received signal is fluctuated with the target moving from bottom to water surface.

In order to achieve the general principles, a 1 m×1 m aluminum plate with 0.5 cm in thickness is also used. The plate moves vertically in the tank. The amplitude of received signal is 0.55 V without the plate. And the received signals with plate moving are shown in Figs. 8(c) and 8(d). The signals are weakest when the plate goes through the baseline. When the plate is apart from the baseline, the forward scattering signal and the direct signal interfere constructively, and the received signals become stronger.

In both Fig. 4 and Fig. 8, the fluctuation of received signal varies significantly when the target becomes close to baseline. As shown in Fig. 8, the acoustical shadow zone is generated in the near field, owing to the forward scattering, while in the far field, the received signal becomes stronger. When the target moves far from the baseline, the received signal is still fluctuated. This is because forward scattering has sidelobes and the Fresnel spot is generated on the plate vertical to the forward scattering direction.

## 4. Conclusions

The physical principle of the underwater target scattering can provide important theoretical support for target detection. Derived in the paper are scattering function and target strength of a typical cylindrical shell based on the finite cylinder scattering model. A simple experiment is designed and carried out. The forward and the backward target strengths are measured, where the target is insonified by a 30 kHz incident wave using pulse compression technology. The scattering model and measurement results show the following physical phenomena. (i) The forward target strength of the cylindrical shell is much stronger than the backward target strength. Both the simulation and the measurement results show that the forward target strength is 12dB higher than the backward target strength. (ii) In the yaw angle interval $[-45°, 45°]$, the forward target strength varies with yaw angle of target less significantly than that of the backward target strength. (iii) When the target moves beyond the baseline, the Fresnel spot is generated because of the interference between the direct signal and the forward scattering signal. The received signal fluctuates with target moving. When the target approaches the baseline, the acoustical shadow zone is generated in near field and the received signal strength is enhanced in the far field. (iv)The target strengths measured in the near field are 2dB smaller than the model results, which need to be corrected.

In the real application of forward scattering, the forward scattering signal is difficult to observe directly, which is influenced by noise and multi-path transmission. The methods to suppress the direct wave and detect the forward scattering signal need to be further studied.

## References


[1] Zhuo L K, Fan J and Tang W L 2007 *Acta Acoustica* **32** 411 (in Chinese)
[2] Sun Y and Xu H T 2007 *Acta Acoustica* **32** 369 (in Chinese)
[3] Ye Z 1997 *J. Acoust. Soc. Am.* **102** 877
[4] Schmidt H 2004 *Proceeding of High Frequency Ocean Acoustics Conference* California, USA, March 1–5, 2004 p456
[5] Bowman J J, Senior T B A and Uslenghi P L E 1987 *Electromagnetic and Acoustic Scattering by Simple Shapes* (New York: Hemisphere Publishing Corp.) p362
[6] Ingentio F 1987 *J. Acoust. Soc. Am.* **82** 2051
[7] Makris N C 1998 *J. Acoust. Soc. Am.* **104** 2105
[8] Zverev V A, Korotin P I, Matveev A L , Mityugov V V, Orlov D A Salin B M and Turchin V I 2001 *Acoustical Physics* **47** 184
[9] Matveev A L, Spindel R C and Rouseff D 2007 *IEEE Journal of Oceanic Engineering* **32** 626
[10] Gillespie B, Rolt K and Edelson G 1997 *Proceeding of the 23*rd *International Symposium on Acoustical Imaging* Boston April 13–16, 1997 p501
[11] Hollett R D, Kessel R T and Pinto M 2006 *Proceedings of UDT Europe 2006* Hamburg, Germany, June 27–29, 2006 ADA454750
[12] Bertrand A and Josse E 2000 *ICES J. Mar. Sci.* **57** 1143
[13] Hui J, Wang Z J, Hui J Y and He W X 2009 *Acta Phys. Sin.* **58** 5491 (in Chinese)
[14] Tang L G, Xu X M and Liu S X 2008 *Acta Phys. Sin.* **57** 4251 (in Chinese)
[15] Ding L 1997 *J. Acoust. Soc. Am.* **101** 3398
[16] Ding L, Takao Y, Sawada K, Okumura T, Miyanohana Y, Fursusawa M and Farmer D M 1998 *J. Acoust. Soc. Am.* **103** 3241
[17] Fawcett J A 1996 *J. Acoust. Soc. Am.* **100** 3053
[18] Zhu Y 1990 *Principle of Active Sonar Information Detection* (Beijing: Ocean Press) p73 (in Chinese)
[19] Wang D Z and Shang E C 1981 *Underwater Acoustics*( Beijing: Science Press) p351 (in Chinese)
[20] Urick R J 1983 *Principles of Underwater Sound* (3rd ed) (New York: McGraw-Hill) pp312–314